Binding Behavior of Lysine-Containing Helical Peptides to DNA Duplexes Immobilized on a 27 MHz Quartz-Crystal Microbalance

Kenichi Niikura, Hisao Matsuno, and Yoshio Okahata*[a]

Abstract: Binding behavior of alanine-based oligopeptides containing four or six cationic lysine residues (K4 and K6) to a $dA_{30}-dT_{30}$ or $dG_{30}-dC_{30}$ duplex-immobilized on a 27 MHz quartz-crystal microbalance (QCM) were studied in an aqueous buffer solution. Eight kinds of alanine-based oligopeptides were prepared systematically, in which positions of K residues were changed in the helical structure according to common features in DNA recognition helices of the DNA binding protein. The binding amount (Δm) on a nanogram scale and binding constant (K_a) could be obtained from frequency decreases (mass increases) of the DNA-immobilized QCM. Cationic oligopeptides were confirmed, from circular dichroism (CD) spectra, to form α-helical conformations as a result of the binding to DNA strands with random conformations. Δm and K_a values were greatly affected by ionic strength and the position of cationic K residues of peptides. At the low ionic strength, all peptides can bind with the almost same affinity to DNA strands by electrostatic interactions. At the high ionic strength of 40 mM NaCl, oligopeptides with cationic K groups at the one side of the α helix showed larger Δm_{max} (35 ± 5 ng cm^{-2}) and K_a values (10^4 M^{-1}) than those of oligopeptides having K groups in random positions ($\Delta m = 10 \pm 5$ ng cm^{-2} and $K_a = 10^3$ M^{-1}).

Keywords: DNA recognition · lysine · oligomers · peptides · quartz-crystal microbalance

Introduction

It is important to know how proteins recognize the specific sequence of double-stranded DNA in a gene transcription process. To date, X-ray crystallographic studies revealed that the sequence-specific DNA binding proteins such as transcription factors have some similar DNA binding domains. Many of these domains are classified to helix-turn-helix,[1] Zn finger,[2] basic region helix-loop-helix,[3] and basic region leucine zipper.[4] Suzuki[5] predicted from X-ray crystallographic studies that those DNA binding motifs have a common DNA recognition helix, in which cationic lysine (K) or arginine (R) residues at one side of the helix interact with a major groove of DNA strands, and hydrogen-bonding residues such as asparagine (N) and serine (S) at the same site are involved in the selective recognition of DNA nucleobases (see Figure 1A).

In addition to the static X-ray crystallographic studies of DNA-peptide interactions, several papers report on studies into the dynamic interactions between DNA strands and cationic oligopeptides containing basic amino acid residues at specific positions.[6] However, they did not focus on the common position of basic amino acid residues and did not give the relationship between the position and their binding constants. The binding behavior of proteins or peptides to DNA has been studied mainly by gel-mobility shift assay.[7] This technique is widely used in molecular biology; however, it is difficult to detect the binding of small oligopeptides to small fragments of DNA and to evaluate quantitatively the binding process and amount. Usually basic peptides containing lysines form a random structure due to the coulombic repulsion between basic amino acid residues and form an α-helical conformation after binding to DNA strands as a result of the interaction with phosphate groups. Therefore, the binding properties of these cationic oligopeptides to DNA can be followed by the increase of α-helical content by circular dichroism (CD) spectroscopic measurements or by changes in the fluorescent spectra of tryptophan residues.[6] However, CD or fluorescent spectra changes are not quantitative if the formation of helical structures is not proportional to the amount of DNA binding, and it is difficult to obtain the absolute binding amount of oligopeptide to DNA. In order to provide general rules on how helical peptides bind to a major groove of DNA strand, systematic and quantitative studies are achieved by the use of a new detection technique.

In this paper, we report quantitative studies of the binding behavior of basic α-helical oligopeptides to a $dA_{30}-dT_{30}$ or $dG_{30}-dC_{30}$ duplex immobilized on a highly sensitive 27 MHz

[a] Prof. Y. Okahata, Dr. K. Niikura, H. Matsuno
Department of Biomolecular Engineering
Tokyo Institute of Technology
Nagatsuda, Midori-ku, Yokohama 226–8501 (Japan)
Fax: (+81) 45-924-5836
E-mail: yokahata@bio.tietech.ac.jp

  0947-6539/99/0505-1609 $ 17.50+.50/0

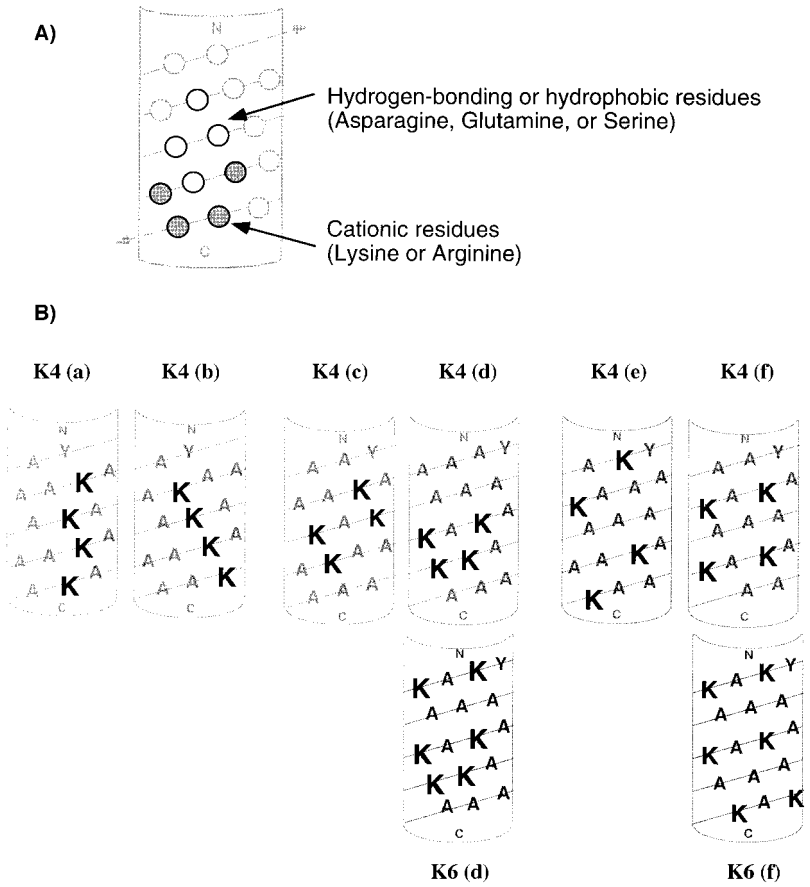

Figure 1. A) A cylindrical structure of common features of the DNA recognition helix (see ref. [5]). B) Cylindrical structures of cationic lysine (K)-containing alanine (A)-based oligopeptides (16–17 mer). Tyrosine (Y) was introduced at the N terminal for easy detection by UV absorption, and the C and N terminals were acetylated and amidated, respectively.

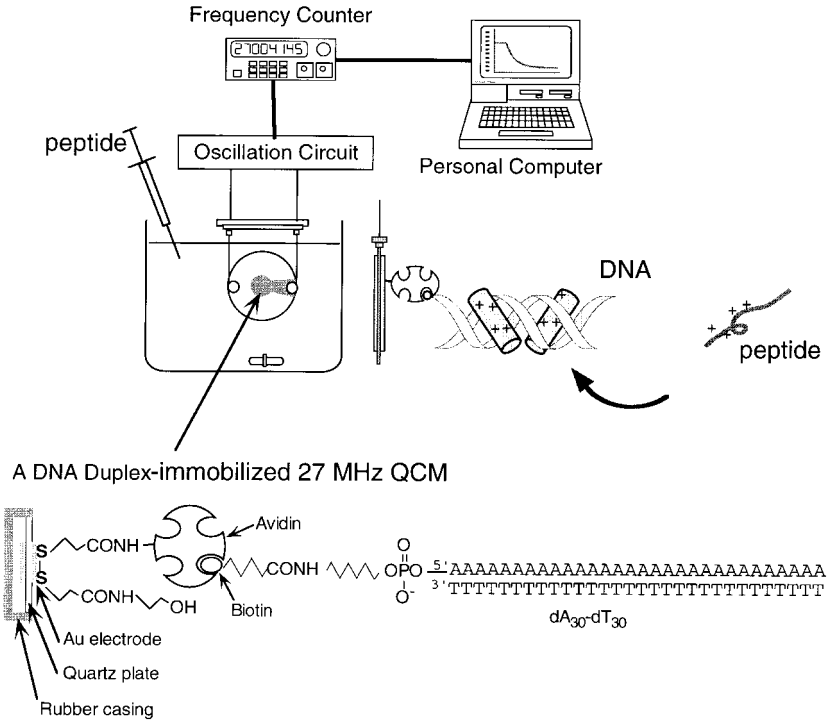

Figure 2. A schematic illustration of a 27 MHz QCM measurement system and chemical structures of immobilized DNA strands on the Au electrode (4.9 mm^2 area) of the QCM.

QCM in an aqueous solution (Figure 2). A QCM is known to provide very sensitive mass measurements in an aqueous solution,[8, 9] as well as in gas phase,[10, 11] because its resonance frequency decreases linearly upon the increase of a mass on the QCM electrode in the nanogram range.[12] From time courses of frequency decreases (mass increases) due to the binding of oligopeptides to the DNA-immobilized QCM, the binding amount (Δm), at a nanogram level, and binding constant (K_a) could be obtained. In order to investigate the role of electrostatic interaction for the DNA binding peptide, we have designed eight kinds of alanine-based 16–17 mer peptides containing four or six cationic lysine (K) residues; in these peptides the position of K residues are systematically changed. Cylindrical structures of prepared oligopeptides are shown in Figure 1B. K4(a)–K4(f), K6(d), and K6(f) oligopeptides have four or six K residues at different positions. The N and C terminals were acetylated and amidated, respectively, and one tyrosine (Y) at the N terminal was introduced for the easy detection by UV absorption during preparations and purification of peptides. We[9,11] and other researchers[8, 10] have used 5–9 MHz QCMs as a molecular detector for a biosensor. The 27 MHz QCM used in this study is about 10 times more sensitive than our conventional 9 MHz QCM,[13] and has a mass change sensitivity of 0.6 ng cm^{-2} per 1 Hz of frequency decrease.[13,14] This sensitivity is enough to detect a mass change of 10–50 ng cm^{-2} obtained by the binding of relatively small 16–17 mer oligopeptide to DNA. Ward and coworkers have demonstrated that a 30 MHz QCM can be operated in the liquid phase.[8g]

0947-6539/99/0505-1610 $ 17.50+.50/0 *Chem. Eur. J.* **1999**, *5*, No. 5

Results

Immobilization of DNA strands: A schematic representation of the immobilization of $dA_{30}-dT_{30}$ strands is shown in Figure 2, according to our previous paper.[15, 16] First, avidin molecules were covalently bound to carboxyl groups on the one side of Au electrodes (4.9 mm^2) of a 27 MHz QCM; the other side of Au electrodes was sealed with a rubber casing to avoid contact with buffer solution (see Experimental Section).[13–16] The presence of a monolayer of avidin molecules on the surface of the electrode was confirmed by the frequency decrease (mass increase) of the QCM (480–600 $ng\,cm^{-2}$, 7×10^{-12} $mol\,cm^{-2}$).

We also tried to immobilize avidin by physical adsorption on a bare Au electrode.[8e] However, the physically adsorbed avidin layer was not so stable as to get constant results and was not suitable for re-use, compared with our covalently bound avidin layer. Biotinylated dA_{30} hybridized with dT_{30} was immobilized on the covalently bound avidin layer on the QCM surface by immersing the QCM for about 30 min. in the aqueous buffer solution of DNA (120 ± 3 $ng\,cm^{-2}$, ca. 6×10^{-12} $mol\,cm^{-2}$). The biotinylated $dA_{30}-dT_{30}$ strand (3.2 nm^2 area per molecule) can be calculated to cover about 15% of the Au electrode (area: 4.9 mm^2), and it binds to one of four binding sites of an avidin molecule. The immobilized amount of DNA strands on the QCM was controlled so that the coverage was about 15% in order to keep the enough space for oligopeptide binding. The immobilized amount of DNA strands on the QCM could be controlled from 10 to 80% by the immersing period.

The $dG_{30}-dC_{30}$ strands could be also immobilized on a QCM in the same amount in the same manner, instead of $dA_{30}-dT_{30}$ strands.

Design of peptides: As shown in Figure 1B, six kinds of K4 peptides in which four basic lysine residues exist at different positions in cylindrical forms were prepared, as well as two K6(d) and K6(f) peptides with two additional K residues to the K4(d) and K4(f) peptides, respectively. K4(a) and K4(b) have four K groups perpendicular in the one side of a cylindrical form. K4(c) has two lines of K groups, and K4(d) has the four K groups in a v-shape formation, imitating naturally occurring sites. K6(d) has two additional K groups at the top of a v-shape formation, mimicking the cationic position of bZIP peptide, one of typical DNA binding motifs.[4, 5] Lysine groups in these peptides were confirmed, from computer-aided CPK molecular modeling, to align on one side of peptide helix (see Figure 8). In contrast, the lysine groups in K4(e), K4(f), and K6(f) are placed at random in the α helix. The reason why alanine-based 16–17 mer peptides were chosen as a simple helical peptide is that alanine can form stable helical structures even in a short peptide.

Time courses of peptide binding: Figure 3A shows typical time courses of frequency decreases (mass increases) of the $dA_{30}-dT_{30}$ (or single-stranded dA_{30}-immobilized 27 MHz QCM) in response to the addition of K4(a) and K4(f) peptides in the aqueous solution at 10 °C and pH 7.5, and with 10 mM phosphate and 20 mM NaCl. The binding reached

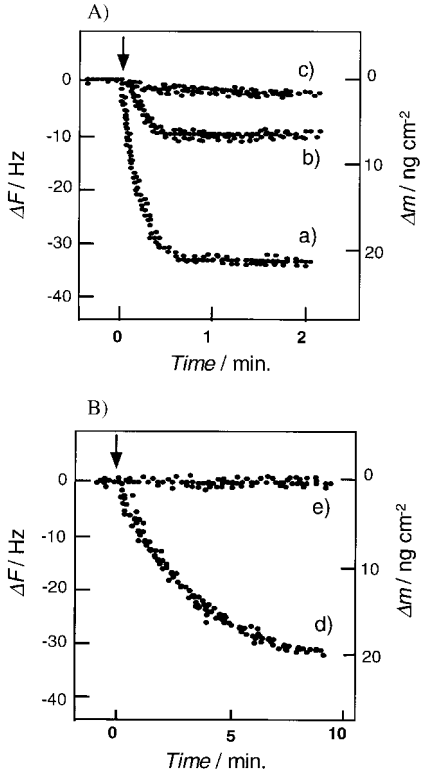

Figure 3. Typical time courses of frequency decreases (mass increases) of a $dA_{30}-dT_{30}$ or a single-stranded dA_{30}-immobilized 27 MHz QCM responding to the addition of A) K4 peptides and B) K6 peptides in the aqueous solution. a) $dA_{30}-dT_{30}+K4(a)$; b) $dA_{30}-dT_{30}+K4(f)$; c) dA_{30} (a single strand) + K4(a); d) $dA_{30}-dT_{30}+K6(d)$; e) $dA_{30}-dT_{30}+K6(f)$; (10 °C, pH 7.5, 10 mM phosphate, 20 mM NaCl, [K4] = 5 μM, [K6] = 2 μM).

equilibrium within 1 min, and the larger mass increase was observed for the injection of K4(a) peptide, in which four K groups aligned perpendicularly in the cylindrical structure, than that for K4(f) peptide with four K groups at random positions. Binding behavior was greatly dependent on the position of cationic K groups in the K4 peptides. These peptides showed similar binding behavior with the $dG_{30}-dC_{30}$ strands: K4(a) bound with $\Delta m=20\pm5$ $ng\,cm^{-2}$ within 1 min, but K4(f) showed a small amount of binding with $\Delta m=6\pm2$ $ng\,cm^{-2}$; these results are very similar to those for the $dA_{30}-dT_{30}$. Since these simple basic peptides did not show any significant binding difference for AT or GC strands, the $dA_{30}-dT_{30}$ strands were used for the following experiments. Although raw data for binding to the $dG_{30}-dC_{30}$ strands are not shown, the obtained maximum binding amounts (Δm_{max}) and binding constants (K_a) are summarized in Table 1. In Figure 3A, the curve (c) shows the binding of K4(a) peptide to a dA_{30} single strand immobilized QCM. The K4 and K6 peptides did not bind to a single strand DNA. This indicates that a simple electrostatic interaction between cationic peptides and a single strand DNA as polyanions is not important, and that the double helical structure forming a major groove is important as a binding site for peptides. As control experiments, peptides were confirmed to hardly bind to avidin layers without DNA strands on the QCM.

Similar selective binding behavior was also observed for K6 peptides (see Figure 3B). K6(d), with six K residues in a v-shape formation at the one side of the helix, also showed a

Table 1. Maximum binding amounts (Δm_{max}) and association constants (K_a) of K4 and K6 peptides to $dA_{30}-dT_{30}$ or $dG_{30}-dC_{30}$ strands immobilized on a 27 MHz QCM.[a]

	Δm_{max} [ng cm^{-2}]			K_a [10^3 M^{-1}]			α-Helical content at 20 mM NaCl		
	[NaCl] = 0 mM	20 mM	40 mM	[NaCl] = 0 mM	20 mM	40 mM	without DNA	with [DNA] = 10 μM	ratio
K4(a)	46 ± 3	44 ± 3	35 ± 3	790 ± 40	190 ± 20	18 ± 2	18 ± 5	40 ± 5	2.2
	–	38 ± 2[b]	–	–	20 ± 5[b]				
K4(b)	–[c]	–[c]	40 ± 5	–[c]	–[c]	10 ± 2	20 ± 5	34 ± 5	1.7
K4(c)	55 ± 2	28 ± 2	29 ± 5	550 ± 80	170 ± 30	23 ± 2	33 ± 5	60 ± 5	1.8
	–	30 ± 5[b]	–	–	20 ± 3[b]				
K4(d)	35 ± 5	27 ± 5	20 ± 3	610 ± 90	180 ± 30	12 ± 1	35 ± 5	48 ± 5	1.4
–	–	20 ± 5[b]	–	–	12 ± 1[b]				
K4(e)	31 ± 5	31 ± 2	11 ± 3	600 ± 60	64 ± 3	1.6 ± 0.2	32 ± 5	37 ± 5	1.1
	–	11 ± 3[b]	–	–	1.5 ± 0.3[b]				
K4(f)	29 ± 4	24 ± 3	< 10	130 ± 20	30 ± 2	< 1	37 ± 5	42 ± 5	1.1
K6(d)	–	–	40 ± 5	–	500 ± 50	110 ± 10	10 ± 3	30 ± 5[d]	3.0
K6(f)	–	–	< 5	–	< 10	< 3	29 ± 5	33 ± 5[d]	1.1

[a] 10 °C, pH 7.5, 10 mM phosphate. [b] Binding results for $dG_{30}-dC_{30}$ strands. [c] Addition of K4(b) peptide to $dA_{30}-dT_{30}$ strands resulted in the frequency increase (mass decrease) in 0 and 20 mM NaCl. This is explained that K4(b) peptide binds electrostatically to DNA and causes a large conformation change (shrinking) of DNA strands and the mass apparently decreases. Therefore, it is difficult to calculate the binding amount from frequency changes. [d] [DNA] = 2 μM.

large binding to DNA strands, but not K6(f), with K residues in random positions. The K6(d) peptide mimics the cationic positions of bZIP peptide, one of typical DNA binding motifs.[4, 5]

Effect of salt concentration: Figure 4 shows the effect of concentration of NaCl on the K4(a) peptide binding to the $dA_{30}-dT_{30}$ on the QCM. When the NaCl concentration is

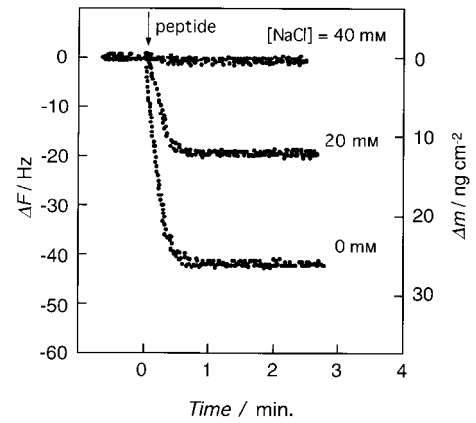

Figure 4. Effect of salt concentrations on the binding behavior of the K4(a) peptide to a $dA_{30}-dT_{30}$ strand (10 °C, pH 7.5, 10 mM phosphate, [K4(a)] = 2 μM).

increased from zero to 40 mM in the 10 mM phosphate buffer solution, the K4(a) binding decreased considerably owing to diminished electrostatic interactions between cationic K4 peptides and anionic DNA phosphates. When the injected concentration was increased to 400 μM, specific binding was observed depending on concentrations even at the 40 mM NaCl concentration.

Maximum binding amount and binding constant: Binding amounts (Δm) showed simple saturation curves against peptide concentrations in phosphate buffer at three different NaCl concentrations (0, 20, and 40 mM) as shown in Figure 5.

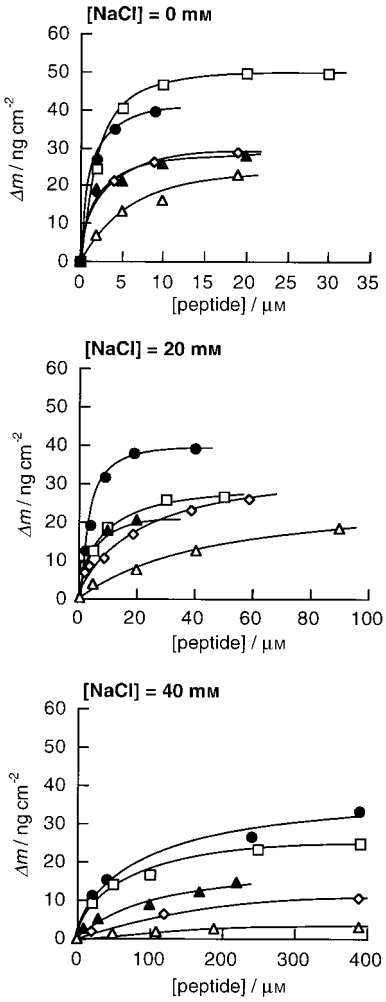

Figure 5. Binding amounts of K4 peptides onto $dA_{30}-dT_{30}$ strands as a function of peptide concentrations at [NaCl] = 0, 20, and 40 mM. ● K4(a), □ K4(c), ▲ K4(d), ◇ K4(e), and △ K4(f), (10 °C, pH 7.5, 10 mM phosphate).

These saturation binding behaviors are expressed as linear correlations by Equation (1) as a reciprocal plot between [peptide]/Δm and [peptide]. Binding constants (K_a) and

0947-6539/99/0505-1612 $ 17.50+.50/0 Chem. Eur. J. 1999, 5, No. 5

$$\frac{[\text{peptide}]}{\Delta m} = \frac{[\text{peptide}]}{\Delta m_{\max}} + \frac{1}{\Delta m_{\max} K_a} \quad (1)$$

maximum binding amount (Δm_{max}) of K4 peptides to $dA_{30}-dT_{30}$ strands were calculated from the slope and intercept of Equation (1), respectively. Δm_{max} and K_a values at different NaCl concentrations are summarized in Table 1, together with the binding results for the $dG_{30}-dC_{30}$ strands.

The saturation binding behavior of the peptides K6(d) and K6(f) to $dA_{30}-dT_{30}$ at [NaCl] = 40 mM are shown in Figure 6, and the results are also summarized in Table 1.

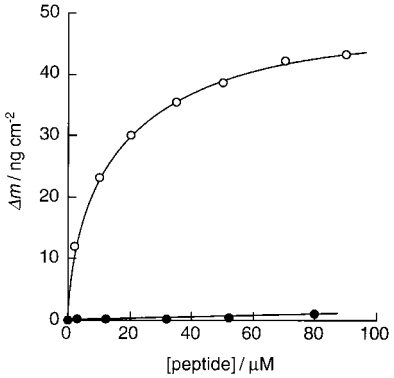

Figure 6. Binding amounts of (○) K6(d) and (●) K6(f) peptides onto $dA_{30}-dT_{30}$ strands as a function of added peptide concentration (10 °C, pH 7.5, 10 mM phosphate, 40 mM NaCl).

CD spectral changes: Binding behavior of K4 or K6 peptides to DNA strands could be also confirmed from CD spectral changes in the bulk solution.[6, 7] Since K4 and K6 peptides have many positively charged K residues as shown in Figure 1B, peptides exist in a random coil conformation in the absence of DNA. When these K4 and K6 peptides bound to DNA strands, they are expected to form an α-helical conformation owing to the interaction with phosphate groups. Figure 7 shows typical difference CD spectra indicating the conformation change of K4(a), K4(f), K6(d), and K6(f) peptides in the absence and presence of $dA_{30}-dT_{30}$ strands in the buffer solution at 20 mM NaCl. CD spectra of peptides with DNA strands were subtracted from that of DNA only. In all cases, no precipitation and turbidity were observed. When DNA strands were added to the peptide solution, the molecular ellipticity at 223 nm (θ_{223}) increased greatly as a reslut of the formation of α-helical structure of the K4(a) and K6(d) peptides. Hippel and coworkers[6a] reported previously changes in CD spectra of the K4(a) peptide upon addition of DNA, and our results are in agreement with this. The α-helical content of peptides could be calculated roughly from θ_{223} values; the θ_{223} value is taken to be $-33\,000$ deg cm^2 dmol^{-1} when peptides exist as 100% α-helical structures.[6a] The percentage of α-helix in peptides in the absence of DNA and in the presence of DNA, and their ratio at 20 mM NaCl are summarized in Table 1.

Discussion

Since 120 ± 3 ng cm^{-2} (ca. 6×10^{-12} mol cm^{-2}) of biotin-$dA_{30}-dT_{30}$ ($M_w = 18\,398$) is immobilized on a QCM, a amss increase

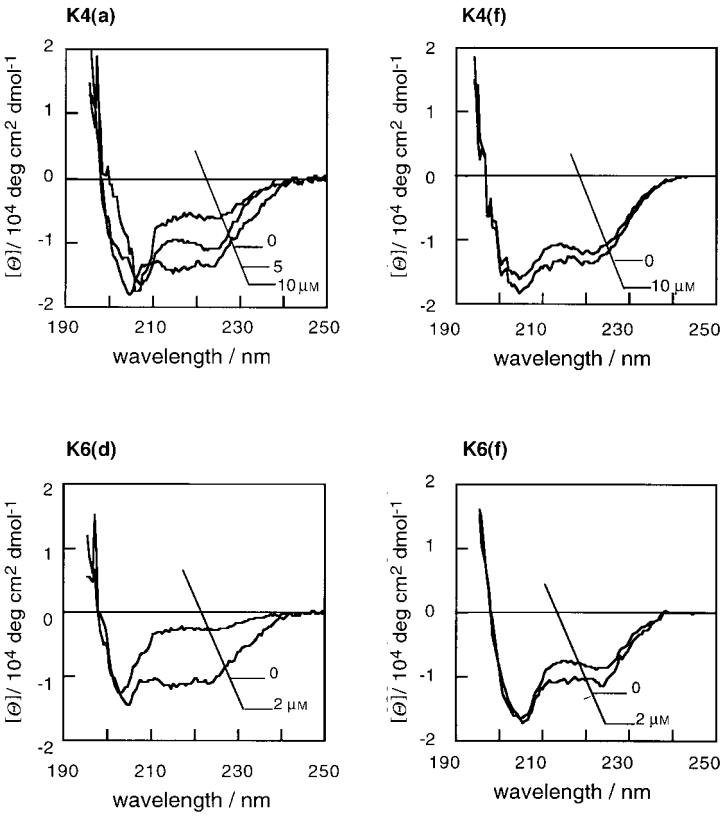

Figure 7. Difference CD spectra of the K4(a), K4(f), K6(d), and K6(f) peptides as a function of the concentration of the $dA_{30}-dT_{30}$ strands. The spectrum of DNA was subtracted from the mixture of DNA and peptide. Concentrations of added $dA_{30}-dT_{30}$ are given in figures. (10 mM phosphate, pH 7.5, 20 mM NaCl, [peptide] = 12 μM).

of about 10–12 ng cm^{-2} is expected if one peptide (Mw = 1510–1702) binds to one DNA strand. In the absence of NaCl (10 mM phosphate buffer), the maximum binding amount (Δm_{max}) of K4 peptides is about 30–55 ng cm^{-2}, which indicates 3–5 peptide molecules bound to one DNA strand (see Table 1). When the NaCl concentration is increased to 40 mM in the solution, Δm_{max} value decreases to 10–40 ng cm^{-2} (1–3 peptides per one DNA) and differed greatly (more than 10 times) depending on the position of K groups in the peptide. A similar tendency was observed in K_a values.

The six K4 peptides can be classified to three groups (see Figure 1B). K4(a) and K4(b) have four K groups perpendicular to a cylindrical structure, and K4(c) and K4(d) have four lysine groups in v-shape formation in the helix. In contrast, K4(e) and K4(f) have lysine groups randomly placed. At low salt concentration, all K4 peptides can bind electrostatically to phosphates of DNA strands regardless of their conformations. However, at high salt concentration, the nonselective electrostatic binding is reduced and multiple interactions between phosphate anions around the major groove of DNA and the cationic K groups on the specific side of the K4(a)–K4(d) peptides become more important. K4 and K6 peptides showed a low affinity to a single strand DNA. This also suggests the above idea. Thus, K4(a)–K4(d) peptides with cationic groups preferentially at the one side of the helix showed larger Δm_{max} (20–40 ng cm^{-2}) and K_a values (1×10^4 M^{-1}) than those of K4(e) and K4(f) with cationic groups

scattered around the helix ($\Delta m_{max} = 10-11$ ng cm^{-2} and $K_a = 1 \times 10^3$ M^{-1}) (see Table 1).

Padmanabhan and coworkers have investigated the binding behavior of K4(a) and K4(e) peptides with calf thymus DNA in the different salt concentration (6.4–21.5 mM) from changes in CD and fluorescent spectra.[6b] The binding constants that they obtained for K4(a) and K4(e) with calf thymus DNA are very close to our QCM data, but the effect of salt concentration is different depending on the peptides. Their results showed that the binding constants decreased with increasing NaCl concentration independent on the K position in the K4(a) and K4(e) peptides. Our QCM results indicate that the binding constants for K4(a)–K4(d) do not decrease much with increasing NaCl concentration, but that those of K4(e) and K4(f) decrease considerably. This difference reflects the selectivity at the high NaCl concentration depending on the position of K groups in peptides. We assume that the QCM method is more sensitive and suitable for these quantitative binding measurements than the spectral method.

α-Helical contents of K4(a) and K4(b) peptides are very small (18–20%) due to the strong electrostatic repulsion between perpendicular aligned cationic groups. K4(c) and K4(d) or K4(e) and K4(f) peptides exist as a helical structure in 32–37%; this is probably a result of the weak repulsion of K4 groups in v-shape or random positions. In the presence of $dA_{30}-dT_{30}$ strands, the helical contents of K4(a)–K4(d) peptides increased 1.4–2.2 times, but those of K4(e) and K4(f) hardly changed. This means that K4(a)–K4(d) peptides showing the high affinity to DNA strands form α-helical structures as a result of the binding of cationic K4 charges with phosphate anions around the major groove of DNA strands. K4(e) and K4(f) cannot form α helixes because the K4 positions in the cylindrical structure are not suitable to bind to and neutralize the phosphate groups.

Figure 8 shows computer-aided CPK molecular models, in which helical peptides are put in the major groove of $dA_{30}-dT_{30}$ strands to interact cationic K groups with anionic phosphates. K4(a) and K4(d) peptides showing the high affinity to DNA seem to be able to bind three or four cationic groups to the phosphate groups, as shown in arrows. In contrast, cationic groups of K4(e) and K4(f) can not interact with phosphate groups if the peptides form the α-helical structure.

The addition of two cationic K groups at the top of K4(d) peptide is very effective in increaseing the affinity to DNA strands. The K_a value of the K6(d) peptide increased 10 times compared with that of K4(d) peptide (see Tab1e 1, at 40 mM NaCl). Since K_a value of K6(f) peptide hardly changed compared with K4(f), the simple or random increase of two cationic charges is not important in this conformation. Selectivity between K6(d) and K6(f) was increased 30 times in comparison with a tenfold increase between K4(d) and K4(f). The α-helical content of K6(d) peptide also increased in the presence of DNA strands, but not for K6(f). This large increase in the affinity of K6(d) peptide suggests that the additional two lysine groups at the top of the v shape in the cylindrical form are very effective for phosphate binding in the major groove of DNA. The v-shape formation of six lysine groups in the cylindrical structure is similar to the position of the DNA recognition helix of bZIP peptide of GCN4 protein[4] (see Figure 1B).

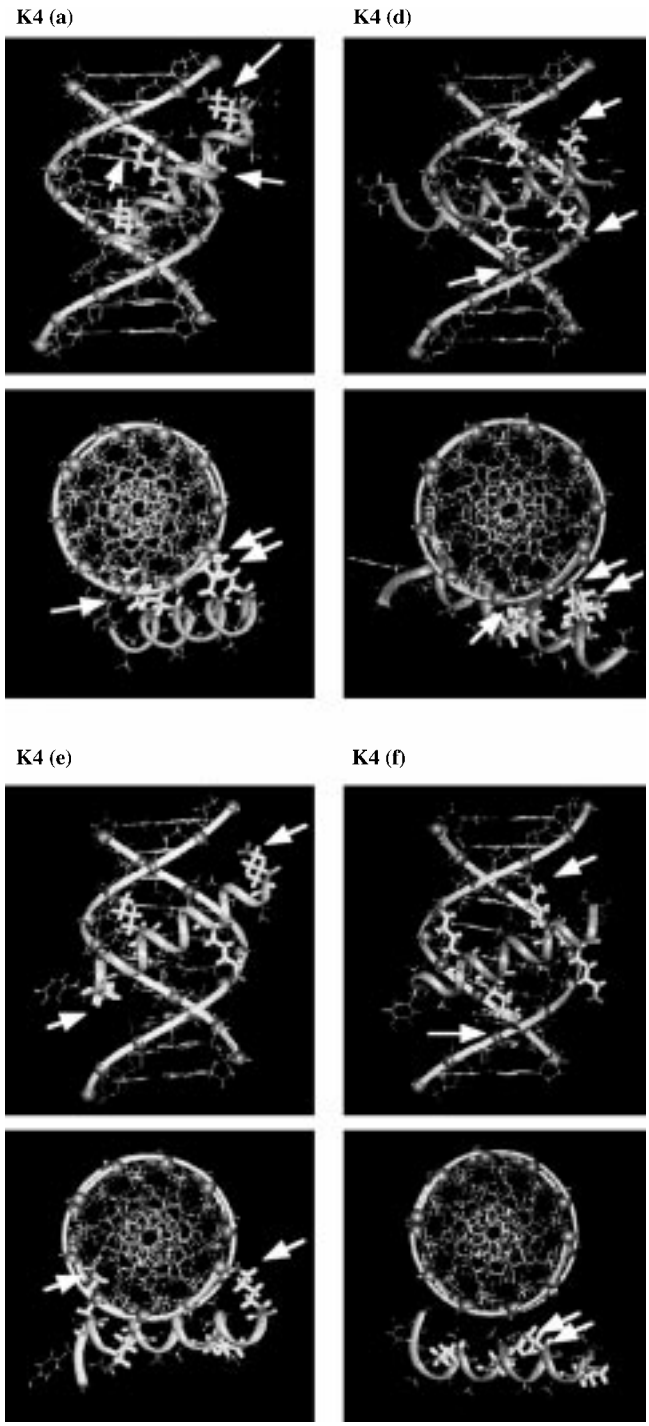

Figure 8. Computer assisted CPK models for interaction of helical K4 peptides with $dA_{30}-dT_{30}$ strands. Whites arrows indicate the strong interaction between a cationic K of peptides and an anionic DNA phosphate.

Conclusion

We synthesized six oligopeptides having 4–6 lysine groups at specific positions. Although the binding affinity did not

0947-6539/99/0505-1614 $ 17.50+.50/0 *Chem. Eur. J.* **1999**, *5*, No. 5

depend on the positiond of K in the peptides at the low ionic solution, the selective binding could be observed at high ionic strength; K6(d), with six K groups at the v-shape formation, showed the highest binding affinity ($K_a = 1 \times 10^5\,\text{M}^{-1}$) to DNA strands. The 27 Hz QCM method is highly sensitive and quantitative for the detection of in situ binding of small helical peptide molecules to DNA strands in the aqueous solution without any labeling. From frequency changes, binding parameters such as maximum binding amount (Δm_{max}) and binding constant (K_a) could be obtained. Since it is otherwise difficult to detect quantitatively binding process and amount of small molecules such as oligopeptides to DNA strands, the QCM technique should become a useful tool for the detection of the binding behavior of DNA-binding peptides.

Experimental Section

Materials: Single-stranded oligonucleotides such as dT_{30} or dG_{30}, and biotinylated dA_{30} or biotinylated dC_{30} were ordered from Pharmacia (Japan). Oligonucleotides were purified with anion-exchange chromatography and their concentrations were determined by an optical-density measurement taken at 260 nm. Peptides were prepared from a single stepwise manual solid-phase peptide synthesis using Fmoc (9-fluorenylmethoxycarbonyl) amino acids: Fmoc-Ala-OH, Fmoc-Lys(Boc)-OH in which the ε-amino group was protected with a *tert*-butyloxycarbonyl group (Boc), and Fmoc-Tyr(*t*Bu)-OH in which the phenoxyl group was protected with a *tert*-butyl group (*t*Bu). Amino acid derivatives were purchased from Watanabe Chemical Industries, Hiroshima. Coupling reactions were performed with 250 mg of Fmoc-NH-SAL resin (0.13 mmol) and Fmoc amino acid (0.4 mmole) in the presence of BOP (0.4 mmole), DIEA (*N*,*N*-diisopropylethylamine) and 1-hydroxybenzotriazole (0.5 mmole) in NMP for 40 min. Completion of the coupling was monitored by Kaiser test, and the coupling reaction was repeated until completion. Removal of Fmoc group was performed by treatment with 20% piperidine-NMP. The amino termini were acetylated with aceticanhydride and the peptides were cleaved from the resin with a cleavage mixture containing thioanisole (1.6 mL) and *m*-cresol (0.24 mL) in trifluoroacetic acid (10 mL). Purification was done by reverse-phase HPLC with a Cosmosil 5C18AR-II column (Nacarai Tesque; 10×250 mm) and a linear gradient of acetonitrile-water with 0.1% trifluoroacetic acid (1 to 60% acetonitrile in 30 min; flow rate: 3 mL min^{-1}). The eluted oligopeptides were then lyophilized. Each peptide was identified by matrix-assisted laser desorption ionization (MALDI) mass spectrometry. Other chemicals were purchased from Tokyo Kasei and Sigma, and used without further purification.

A 27 MHz QCM and it's calibration: A 27 MHz, AT-cut QCM was commercially available from Showa Crystals, Chiba (Japan). The diameter of its quartz plate was 8 mm and Au electrodes were deposited on both sides (diameter: 2.5 mm, area: 4.9 mm^2).[13–16] The one side of the quartz crystal was sealed with a rubber casing, maintaining it in an air environment to avoid contact with the ionic aqueous solution, while the other was exposed to an aqueous buffer solution.[9, 13–16] A cased 27 MHz QCM was connected to an oscillation circuit designed to drive the quartz in aqueous solution. The frequency changes were followed by a universal frequency counter (Hewlett Packard, Tokyo, model 53131A) attached to a microcomputer system (Macintosh Power Book 170, Apple).[9, 13–16] The Sauerbrey equation [Eq. (2)] was obtained for the AT-cut shear mode QCM,[12] in which ΔF is the measured frequency change (Hz), F_0 the fundamental frequency of the QCM (27×10^6 Hz), Δm the mass change (g), A the electrode area (4.9 mm^2), ρ_q the density of quartz (2.65 g cm^{-3}), and μ_q the shear modulus of quartz (2.95×10^{11} dyn cm^{-2}).

$$\Delta F = -\frac{2F_0^2}{A\sqrt{\rho_q \mu_q}}\Delta m \qquad (2)$$

Calibration of the 27 MHz QCM was carried out analogously to the calibration of our conventional 9 MHz QCM.[9, 11] When a certain amount of polymer solution was cast or LB film of lipid monolayers was deposited on the bare Au electrode side of the QCM plate, a linear relationship was observed between deposited amount of mass and frequency decrease of the QCM that was independent of method and chemical compounds. The slope of this curve yielded that a frequency decrease of 1 Hz corresponded to a mass increase of 0.61 ± 0.1 ng cm^{-2} on the QCM electrode.[13–16] Thus, the sensitivity for the mass change of a 27 MHz QCM was increased by about 10 times, in comparison with our conventional 9 MHz QCM ($\Delta m =$ 6.5 ng cm^{-2}).[9, 11] The noise level of the 27 MHz QCM was ± 2 Hz in buffer solution at 20 °C, and the standard deviation of the frequency was ± 5 Hz for 12 h in buffer solution at 20 °C. These values were the same order of magnitude as the conventional 9 MHz QCM.[9, 11]

Immobilization of DNA on a 27 MHz QCM: Immobilization of a biotinylated $dA_{30}-dT_{30}$ to an avidin-bound QCM is schematically shown in Figure 1.[15] The cleaned bare Au electrode side of the QCM plate was soaked into the aqueous solution (3 mL) of 3,3′-dithiodipropionic acid (1 mM) at room temperature, and the frequency decrease was saturated at about 100–150 Hz (mass increase of 60–90 ng cm^{-2}) after 20 min. This means 3,3′-dithiodipropionic acid (area per molecule: 0.4 nm^2) roughly formed a monolayer on the Au electrode (4.9 mm^2). Before drying, the carboxylic acid on the QCM was treated with *N*-hydroxysuccinimide in the presence of water-soluble carbodiimide [1-ethyl-3-(3-dimethylaminopropyl)carbodiimide] in the aqueous solution. The frequency was roughly equilibrated with a the decrease of 50–100 Hz after 30 min. The QCM with the activated carboxyl groups was immersed in 1 mL of the aqueous buffer solution (pH 7.9, 10 mM Tris-HCl, 0.2 M NaCl) of avidin (10 μg, Mw = 68,000). The frequency decrease reached equilibrium at 800–1000 Hz (480–600 ng cm^{-2}) for 1 h. This means that avidin (section area: 80 nm^2) bound as a monolayer to the electrode (25–30 ng on 4.9 mm^2). Avidin was not removed from the electrode after rinsing with aqueous solution several times. Avidin bound nonspecifically to the bare Au electrode, but not to the carboxylic acid-immobilized surface. The binding amount of avidin to the bare electrode is not constant and not stable enough affect the measurements in the following experiments. The QCM was immersed into the aqueous solution (1 mL) of ethanolamine (1M) for 30 min to deactivate the carboxyl group as β-hydroxyethylamide. The avidin-bound QCM was immersed into 1 mL of the aqueous buffer solution (pH 7.9, 10 mM Tris-HCl, 0.2 M NaCl) of biotinylated $dA_{30}-dT_{30}$ or $dG_{30}-dC_{30}$ (1 μM) at 25 °C. After 30 min, when the frequency decreased by abotu 200 ± 3 Hz (mass increase of 120 ± 3 ng cm^{-2}) in about 30 min, the QCM was picked up to control the immobilization amount. The biotinylated $dA_{30}-dT_{30}$ strand was calculated to cover about 15% of the Au electrode and to bind to one of four binding sites of an avidin molecule.

Binding of peptides to DNA strands on a QCM: A $dA_{30}-dT_{30}$- or $dG_{30}-dC_{30}$-immobilized QCM was soaked in 8 mL of aqueous solution (10 °C, pH 7.5, 10 mM phosphate, 0–40 mM NaCl) and the resonance frequency of the QCM was defined as zero position after equilibrium. The stability and the drift of the 27 MHz QCM frequency in the solution were ± 5 Hz for 12 h at 10 °C. The frequency change of the QCM responding to the addition of 10–100 μL of aqueous solution of peptides was recorded with time. The solution was stirred to avoid any effect of diffusion of peptides, and the stirring did not affect the stability and the amount of frequency changes.

Circular dichroism (CD) spectra: Spectra were observed by use of a J-720WI spectropolarimeter (Nippon Bunkou, Tokyo) with a quartz cell (2 mm cell length, 10 °C, pH 7.5, 10 mM phosphate, 20 mM NaCl). At first the CD spectrum of DNA only was observed, and after incubation with peptide for 10 min., the spectrum of peptide–DNA was observed. The CD differential spectrum of peptide was obtained by subtracting the DNA spectrum from the peptide–DNA spectrum.

[1] S. R. Jordan, C. O. Pabo, *Science* **1988**, *242*, 893.
[2] N. P. Pavletich, C. O. Pabo, *Science* **1991**, *252*, 809.
[3] Q. Dong, E. E. Blatter, Y. W. Ebright, K. Bister, R. H. Ebright, *EMBO J.* **1994**, *13*, 200.
[4] T. E. Ellenberger, C. J. Brandl, K. Struhl, S. C. Harrison, *Cell* **1992**, *71*, 1223.
[5] M. Suzuki, *EMBO J.* **1993**, *12*, 3221.
[6] a) N. P. Johnson, J. Lindstrom, W. A. Baase, P. H. von Hippel, *Proc. Natl. Acad. Sci. USA* **1994**, *91*, 4840; b) S. Padmanabhan, W. Zhang, M. W. Capp, C. F. Anderson, M. T. Record, Jr., *Biochemistry* **1997**, *36*, 5193.

[7] T. Morii, J. Yamane, Y. Aizawa, K. Makino, Y. Sugiura, *J. Am. Chem. Soc*. **1996**, *118*, 10011.
[8] a) M. Thompson, C. L. Arthur, G. K. Haliwal, *Anal. Chem.* **1986**, *58*, 1206; b) H. Muramatsu, J. M. Dicks, E. Tamiya, I. Karube, *Anal. Chem*. **1987**, *59*, 2760; c) R. C. Ebersole, M. D. Ward, *J. Am. Chem. Soc*. **1988**, *110*, 8623; d) E. Tamiya, M. Suzuki, I. Karube, *Anal. Chim. Acta* **1989**, *217*, 321; e) R. C. Ebersole, J. A. Miller, J. R. Moran, M. D. Ward, *J. Am. Chem. Soc.* **1990**, *112*, 3239; f) S. Yamaguchi, T. Shimomura, T. Tatsuma, N. Oyama, *Anal. Chem*. **1993**, *65*, 1925; g) Z. Lin, C. H. Yip, I. S. Joseph, M. D. Ward, *Anal. Chem*. **1993**, *65*, 1546; h) H. Ebato, C. A. Gentry, J. N. Herron, W. Mueller, Y. Okahata, H. Ringsdorf, P. A. Suci, *Anal. Chem*. **1994**, *66*, 1683; i) K. Wakamatsu, K. Hosoda, H. Mitomo, M. Ooya, Y. Okahata, K. Yasunaga, *Anal. Chem*. **1995**, *67*, 3336.
[9] a) Y. Okahata, H. Ebato, X. Ye, *J. Chem. Soc. Chem. Commun.* **1988**, 1037; b) Y. Ebara, Y. Okahata, *Langmuir* **1993**, *9*, 574; c) Y. Okahata, K. Ijiro, Y. Matsuzaki, *Langmuir* **1993**, *9*, 19–21; d) Y. Okahata, Y. Matsuzaki, K. Ijiro, *Sensors Actuators B, Chemical* **1993**, *13*, 380; e) Y. Ebara, Y. Okahata, *J. Am. Chem. Soc*. **1994**, *116*, 11209; f) T. Sato, T. Serizawa, Y. Okahata, *Biochem. Biophys. Res. Commun*. **1994**, *204*, 551; g) Y. Okahata, K. Yasunaga, K. Ogura, *J. Chem. Soc. Chem. Commun*. **1994**, 469; h) Y. Okahata, Y. Ebara, *Current Topics in Biophysics*, *Vol. 3* (Eds.: T. Frangopo and M. Sanduloviciu), Iasi University Press (Romania), **1995**, p. 152–171; i) T. Sato, T. Serizawa, Y. Okahata, *Biochim. Biophys. Acta* **1996**, *1285*, 14.
[10] a) G. G. Guilbault, *Anal. Chem*. **1983**, *55*, 1682; b) K. D. Schierbaum, T. Weiss, E. U. T. von Velzen, J. F. J. Engbersen, D, N, Reinhoudt, W. Göpel, *Science* **1994**, *265*, 1413; c) H. C. Yang, D. L. Dermody, C. Xu, A. J. Ricco, R. M. Crooks, *Langmuir* **1996**, *12*, 726; d) M. Wells, D. L. Dermody, H. C. Yang, Y. T. Kim, R. M. Crooks, *Langmuir* **1996**, *12*, 1989; e) J. W. Grate, S. J. Patrash, M. H. Abraham, C. M. Du, *Anal. Chem*. **1996**, *68*, 913.
[11] a) Y. Okahata, H. Ebato, K. Taguchi, *J. Chem. Soc. Chem. Commun.* **1987**, 1363; b) Y. Okahata, K. Kimura, K. Ariga, *J. Am. Chem. Soc*. **1989**, *111*, 9190; c) Y. Okahata, H. Ebato, *J. Chem. Soc. Perkin Trans. 2*. **1991**, 457; d) Y. Okahata, H. Ebato, *Anal. Chem*. **1991**, *63*, 203–207; e) Y. Okahata, H. Ebato, *Trends Anal. Chem*. **1992**, *11*, 344; f) Y. Okahata, *Olfaction and Taste IV* (Eds.: T. Kurihara, N. Suzuki, H. Ogawa), Springer, Tokyo, **1994**, p 703; g) K. Matsuura, Y. Ebara, Y. Okahata, *Thin Solid Films* **1996**, *273*, 61; h) Y. Okahata, K. Matsuura, K. Ito, Y. Ebara, *Langmuir* **1996**, *12*, 1023; i) Y. Okahata, K. Matsuura, Y. Ebara, *Supramol. Sci*. **1996**, *3*, 165; j) K. Matsuura, Y. Okahata, *Chem. Lett*. **1996**, 119; k) K. Matsuura, Y. Ebara, Y. Okahata, *Langmuir* **1997**, *13*, 814.
[12] G. Sauerbrey, *Z. Phys.* **1959**, *155*, 206.
[13] Y. Ebara, K. Itakura, Y. Okahata, *Langmuir* **1996** *12*, 5165–5170.
[14] K. Niikura, K. Nagata, Y. Okahata, *Chem. Lett*. **1996**, 863.
[15] Y. Okahata, M. Kawase, K. Niikura, F. Ohtake, H. Furusawa, Y. Ebara, *Anal. Chem*. **1998**, *70*, 1288.
[16] Y. Okahata, K. Niikura, Y. Sugiura, M. Sawada, T. Morii, *Biochemistry* **1998**, *37*, 5666.

Received: September 14, 1998 [F1343]

  0947-6539/99/0505-1616 $ 17.50+.50/0